RESULTS AND DISCUSSION

CHAPTER 4

CHARACTERISATION OF FOSSIL BONE COATINGS

4.1 Characterization of manganese oxide surface coatings

The characterization of environmental manganese oxide coatings is complex and requires the use of more than one technique. The main objective was to try and determine the dominant mineral phase and elemental composition of the coatings. Poor crystallinity and a large silica dioxide concentration in the coatings present the most problems when trying to characterize these coatings using specific techniques such as Powder X-ray Diffraction (Chukhrov and Gorshkov, 1981).

4.1.1 Elemental and chemical composition of (ICP-OES)

Two fossil bones were lightly rinsed with deionised water in order to remove any loose foreign debris and dust particles from the surfaces. The thick protruding outer dark oxide coating was then carefully removed using a Teflon spatula to avoid contamination. The sample coating was placed in a microwave digestion vessel and digested according to the EPA standard method. The resulting solution was then analyzed using ICP-OES. The results of the two samples are shown in table 4.1 below. It is important to note that the two bone samples were of slightly different shape, size, age and the location in which they were excavated was not identical. These factors can play a major role in determining the elemental composition of the oxide coating. It is for this reason that although the

mineral trends are fairly similar, the absolute mineral concentrations differ considerably for some elements.

Table 4.1 Elemental analysis for two different manganese oxide fossil coatings located on different bone specimens from The Cradle of Humankind.

Fossil bone coating I			*Fossil bone coating II*		
Sample mass		0.1012 g	Sample mass		0.0479 g
Element	**Concentration/ mg L^{-1} (dry mass)**	**SD**	**Element**	**Concentration/ mg L^{-1} (dry mass)**	**SD**
Mg	4 753	0.397	**Mg**	3 841	0.327
Al	41 700	0.465	**Al**	35 762	0.495
Si	56 916	0.27	**Si**	35 647	0.179
P	61 018	0.544	**P**	30 198	1.267
S	101 062	5.645	**S**	278 706	3.272
K	28 409	1.299	**K**	11 242	3.04
Ca	27 372	0.341	**Ca**	19 436	0.643
Ti	3 997	2.915	**Ti**	4 290	4.369
Cr	129	1.598	**Cr**	167	0.787
Mn	111 092	0.386	**Mn**	32 589	0.258
Fe	46 146	0.619	**Fe**	56 994	0.184
Co	95	6.145	**Bi**	48 706	0.733
Ni	402	0.814	**Ni**	79	0.774
Cu	502	1.003	**Cu**	335	0.321
Sr	334	0.835	**Sr**	133	1.075
Ge	265	6.01	**Ge**	214	6.105
Zn	1 705	0.37	**V**	102	3.991

Note: All results in table 4.1 pertain to the thick (approximately 1 mm) dark surface coatings of two different fossil bones. Manganese oxide coatings below were obtained from two different fossil bones, namely samples I and II for comparison.

The manganese to iron ratio for each sample was determined to be 2:1 and 1:2 Mn:Fe for fossil bone coating I and II, respectively. This shows that the manganese: iron ratios could vary from sample coatings originating from different bones. It could perhaps be suggested that for fossil bone coating II, a high bismuth concentration relative to iron and manganese could be a factor in the reduced manganese concentration, relative to the manganese concentration in fossil bone coating I. It has also been observed on a qualitative level that these oxide coatings vary in color and texture for different fossil bone and teeth samples. This could thus substantiate the above results, with lighter red to brown coating containing higher concentrations of iron relative to manganese, and conversely, darker coatings higher concentrations of manganese relative to iron.

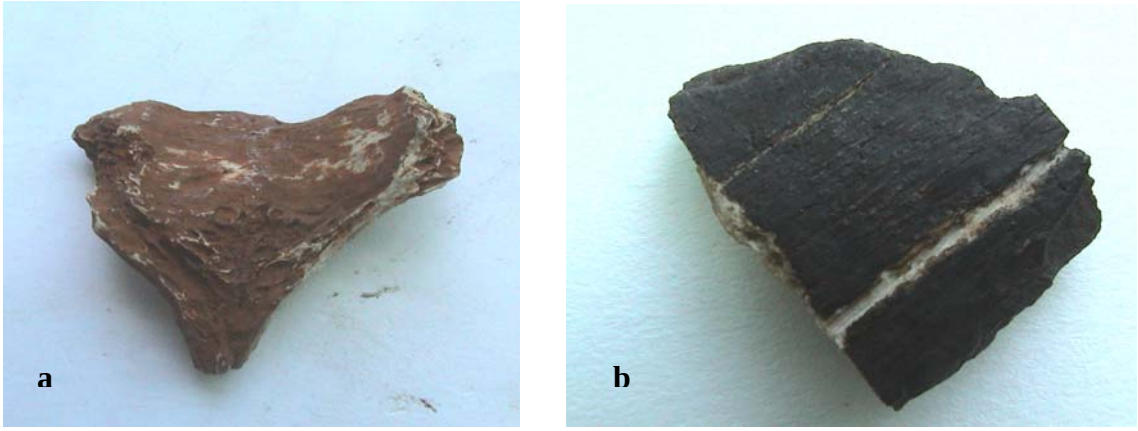

Figure 4.1 Two manganese oxide coated fossil bone fragments differing in colour. **a,** light brown indicating a higher concentration of iron in the oxide coating. **b,** darker brown to black which is indicative of higher manganese concentrations.

In a pilot study conducted prior to the final optimization of the hydrogen peroxide method, a Fe : Mn ratio of the coating was determined to be 1:1.5 for a selected sample. The relatively high manganese content on bone surfaces is indicative of the relatively high abundance of manganese in the dolomites of the Transvaal Super group (Eriksson *et al*., 1975), as well as the more mobile property of Mn compared to Fe in the environment of breccia decalcification.

Manganese oxides have also been found to differ considerably regarding reactivity which is related to their surface properties (surface charge). One reason for this is due to aging of the freshly precipitated manganese oxide mineral into a more stable form. Aging could be due to condensation followed by dehydration of the oxide layer, which could also account for the varying reactivities related to their surface charge (Murray, 1974).

4.1.2 Mineralogical analysis (Powder XRD)

The two main objectives for the use of Powder XRD as a characterization method was to determine the most common crystalline mineral compositions and phases that these oxide coatings share amongst a number of different size and shape samples obtained from different fossil bones and teeth. The coatings were removed from the fossil bones and teeth with great care to ensure that no bone fragments contaminated the coating powder to be analyzed.

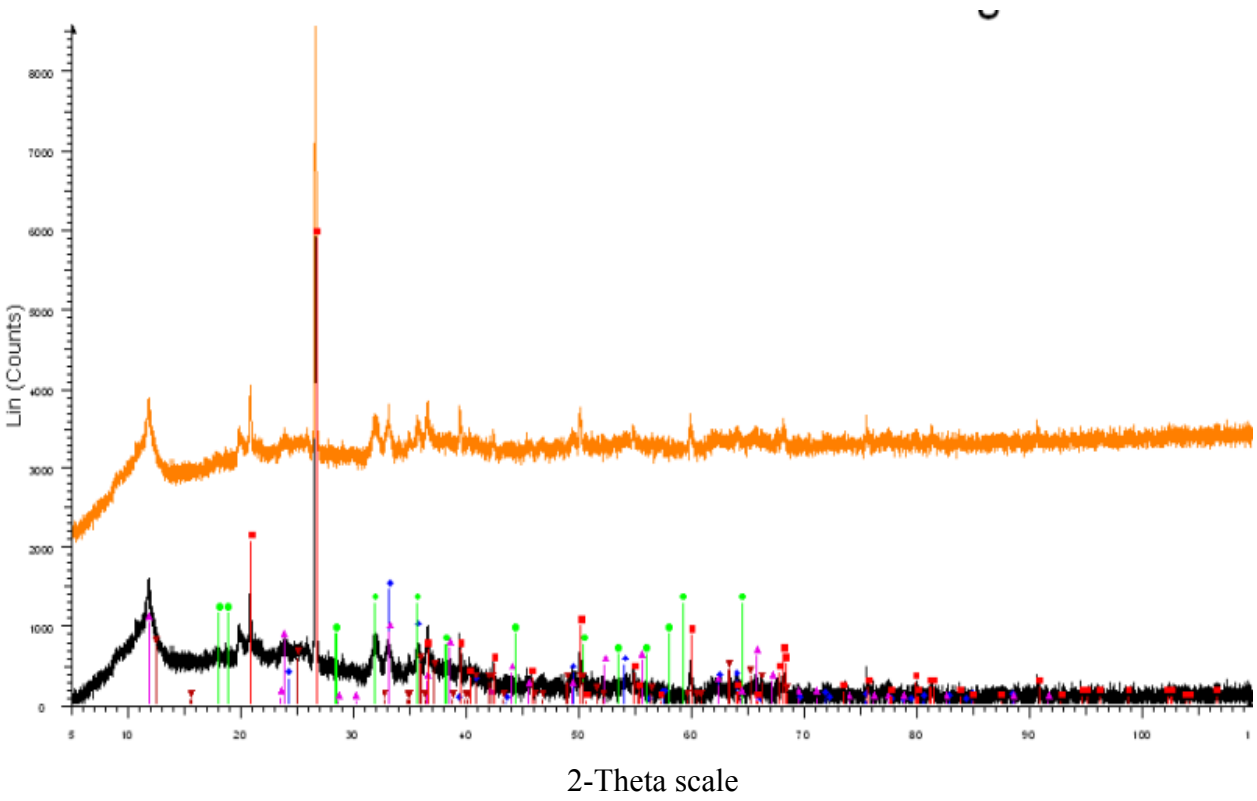

Δ Ramsdelite
□ Quartz alpha hexagonal
◊ Manganese oxide hydrate
◊ Hematite Rhombohedral
□ Background correction
Δ Birnessite

Figure 4.2 Powder XRD pattern for a manganese oxide coated fossil bone showing the superimposed background correction.

In fig. 4.2 two powder XRD patterns are given. The top pattern is a representation for the non corrected background. The second pattern shows a background correction having been performed. These samples typically contain a high percentage of quarts found typically in the matrix where the fossils are found and which have some very intense peaks and a high background noise level that can mask other more important peaks of interest of the mineral phase that is to be determined. The most obvious of the quarts interfering signals is located at a 2-Theta position of approximately 27. Due to the average detection limit of powder XRD being in the region of 2.5%, the quarts prevents accurate analysis of other phases that are found in much smaller percentages relative to the quarts. Some other phases were however determined after a background correction was performed which simplified the search and match process from the data base.

These include: Geothite, Hematite, Manganese oxide (alpha), Rancieite, Birnessite and Ramsdelite.

Powder XRD comparison of several different sample coatings

Five random bone specimens were selected and their coatings removed for XRD analysis to determine if there were any significant different features in mineral phase for different fossil bones.

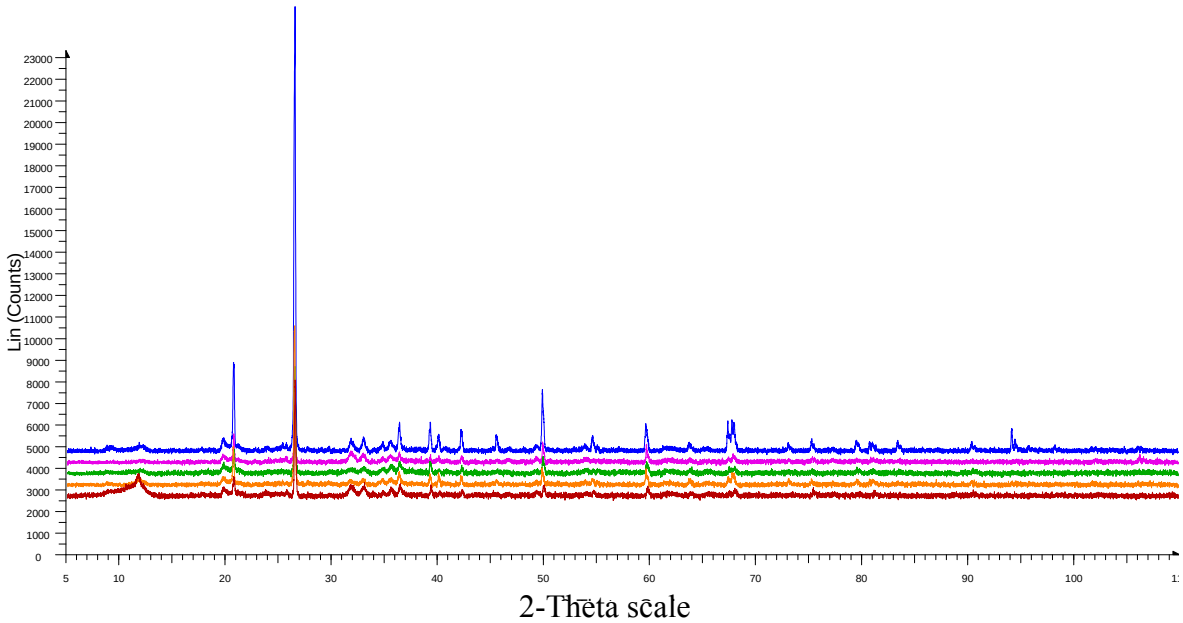

Figure 4.3 Powder XRD pattern obtained for five different fossil bone coatings each originating from different bone fragments.

The above overlaid XRD patterns (fig. 4.3) show five different fossil bone samples all yielding similar peak positions. This shows that the crystal phase for oxide coatings obtained from different fossil specimens are almost identical with respect to mineral phase.

Although there might be other physical and chemical factors that influence the specimen coating's reactivity to the different treatment methods, this shows that the phases of the coatings do not differ considerably enough to have an influence on variability between samples with respect to mass cleaning.

4.1.3 Raman spectroscopy – characterization of oxides

Raman spectroscopy was performed on a number of different fossil bone coatings and for comparison uncoated fossil bone fragments. This analysis was done to determine the

exact nature of the oxide coatings and compare these spectrograms with known synthetic and environmental sample spectrograms.

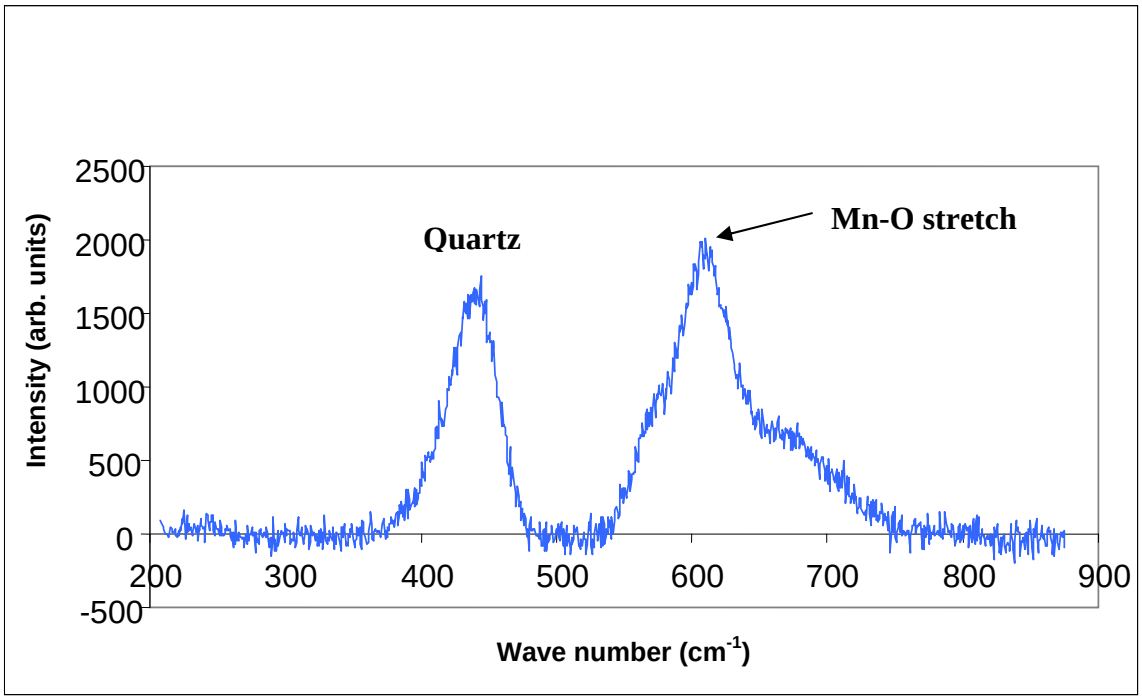

Figure 4.4 Raman spectrum of a thickly coated manganese oxide fossil bone fragment after background subtraction.

There are two main peaks produced, with a third showing overlap with the sample surface of the manganese oxide coated fossil bones. These correspond to the 460 cm^{-1},600 $cm^{-1}$and 675 cm^{-1} wavelength positions. The peak at 460 cm^{-1} is due to the presence of quartz (Burke, 2001; Julien, *et al*., 2003; Liang, *et al*., 2006) on the surface and incorporated in the subsurface of the mineral coating.

The above spectrum also shows similarity to a typical lithiated Birnessite structure with a characteristic peak at 600 cm^{-1}. This is a Mn-O stretching mode of the MnO_6 octahedra

that normally occurs at approximately 605 cm^{-1} due to the greater Mn–O distances (Julien, *et al*., 2003; Julien, *et al*., 2006)

The lithiated birnessite determined as the form of birnessite existing in these manganese oxide coatings could typically consist of a crystal lattice of the arrangement of MnO_6 octahedra with a hexagonal closely packed oxygen lattice providing two different sites for manganese cations, which ensures an open framework structure for easy Li-ion substitution (Julien, *et al*., 2006)

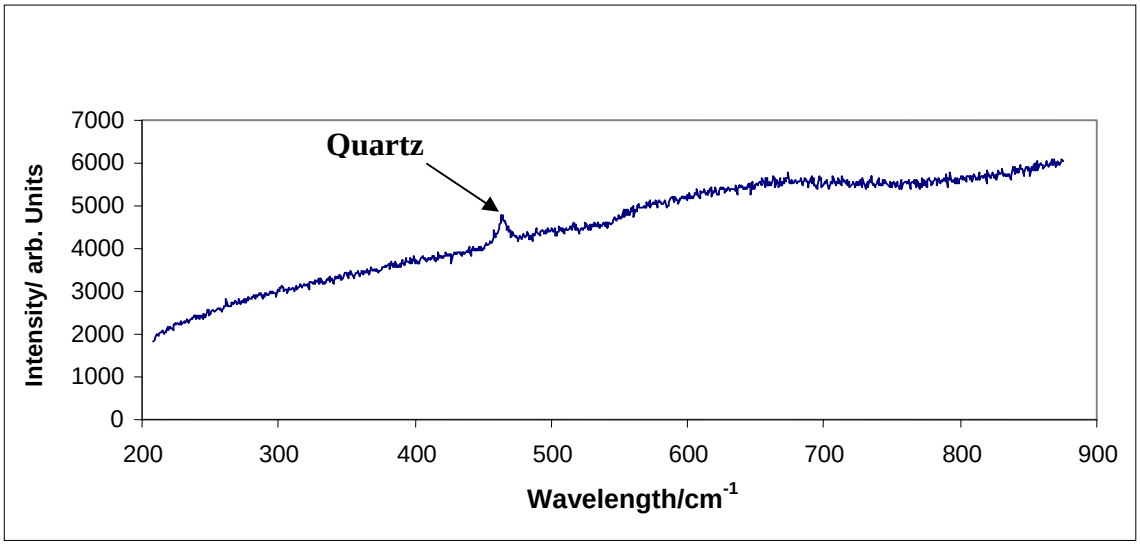

Figure 4.5 Raman spectrum of the interference signals caused as a result of quartz being present in the manganese oxide mineral coatings.

There is an intense quartz peak which can be seen at a wavelength of approximately 460 cm^{-1}. This peak tends to dominate the signal to background noise level and can thus also mask any other peaks produced from the manganese oxide mineral coating.

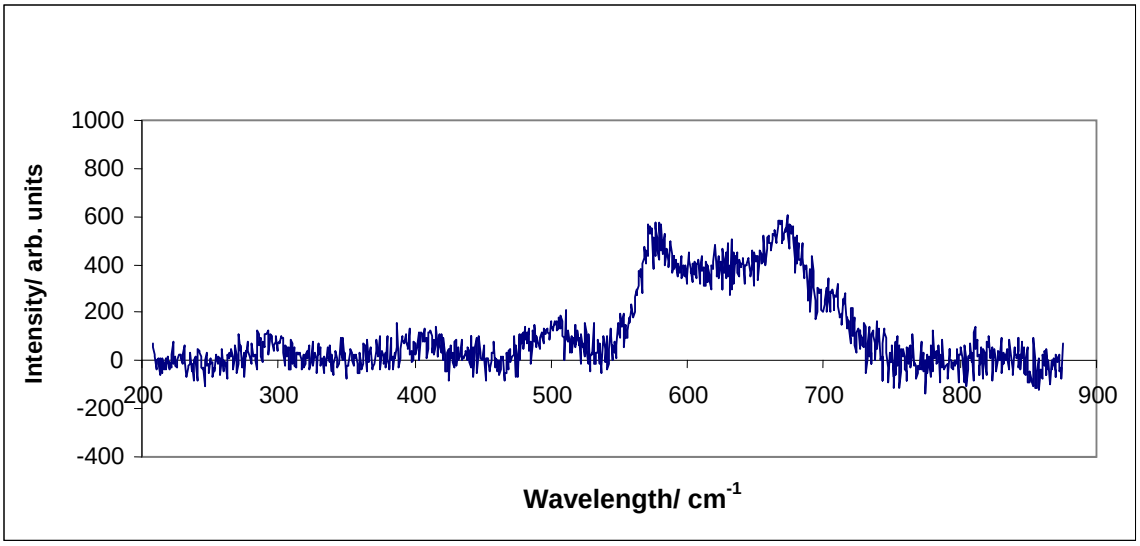

Figure 4.6 Raman spectra showing a weaker signal after background subtraction generated by a manganese oxide coated fossil bone surface.

In figure 4.6 above, a weaker spectrum with visible peak broadening.

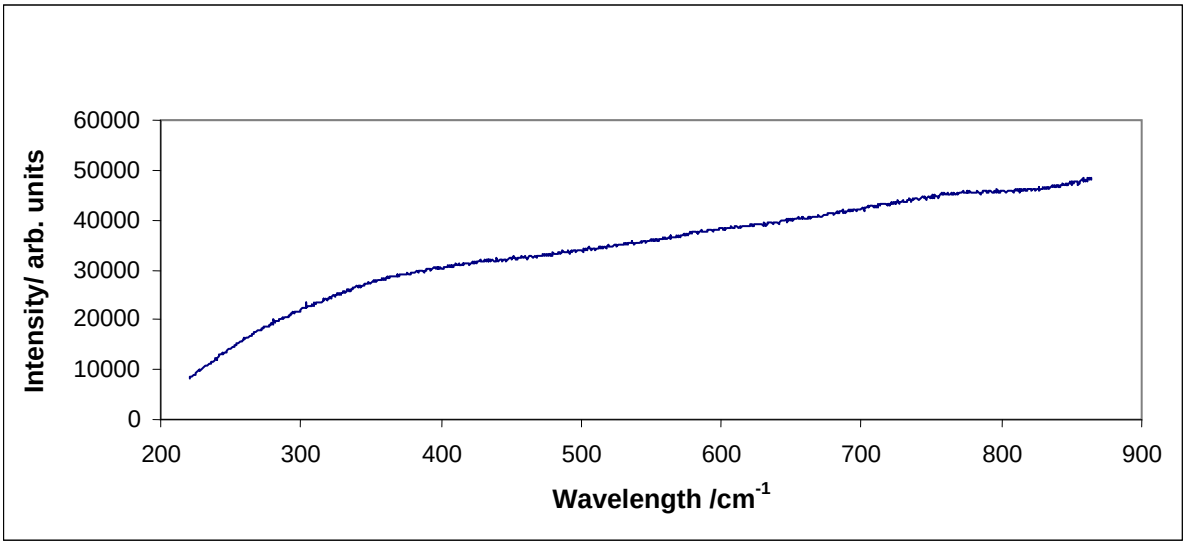

Figure 4.7 Raman spectrum for a clean uncoated fossil bone surface.

In order to differentiate the peaks generated by the manganese oxide coating and the bone itself, a Raman spectrum was run for a clean uncoated fossil bone specimen. It is clear from the above spectrum when compared to both the corrected and uncorrected manganese oxide coated samples that the peaks do not correspond with the spectrum above. There is, however, evidence of a peak corresponding to that of quartz at the 460 cm^{-1} wavelength position.

4.1.4 Infrared spectroscopy

An Infra red spectrum of the manganese oxide bone coating was run in order to determine individual components. It is well known that IR spectra of manganese oxides are mainly dependent on the MnO_6 octahedral framework. Further more, Kang, *et al*. (2007) showed that the band located around 761 cm^{-1} can be assigned to a characteristic adsorbed band of tunnel type manganese oxides. This implies that for different structured manganese oxides there will be a variation in the IR spectrum obtained.

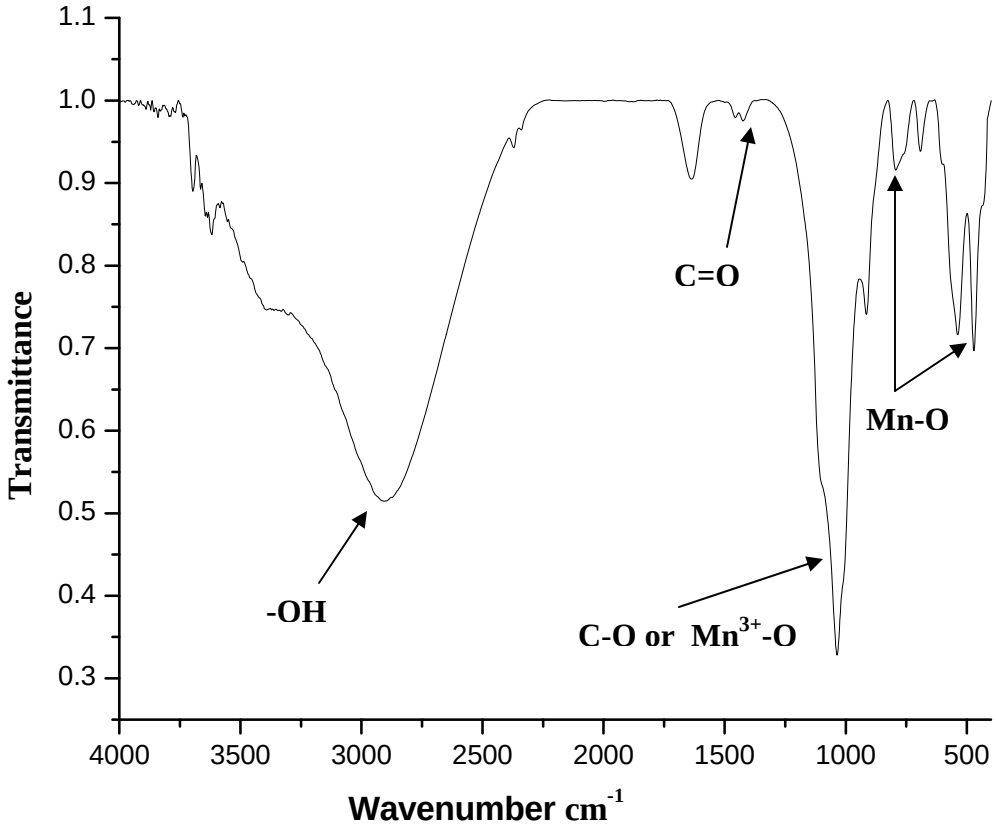

Figure 4.8 Infrared spectrogram of a manganese oxide fossil bone coating.

The above spectrogram, recorded using Infrared (IR) spectroscopy, shows that the fossil bone coating has several components that are IR active. Most of the manganese oxide coatings are amorphous and hydrated. There is a -OH active peak at wave number 2800 cm^{-1} which is from the waters of hydration present in the coating. The peaks at approximately 1600 cm^{-1} and 1050 cm^{-1} show the presence of a C=O and C-O respectively and could be due to the presence of carbonates originating from the bone surface or environment in which the diagenetic processes occurred.

The band at 1050 cm^{-1} could also be assigned to the vibration of the Mn^{3+}-O bond (Farmer, 1975) and this could suggest the major oxidation state of manganese in the structure is not four, or that some Mn^{3+} occupies the Mn^{4+} sites in the crystal lattice of the tunnel structure (Kang *et al*., 2007).

Most bands in the region between 400 cm^{-1} and 800 cm^{-1} could be assigned to Mn–O lattice vibration (Shen and Clearfield, 1986; Feng, *et al*., 1992), the position and intensity of these characteristic adsorbed bands, and thus peaks, located at wave lengths of 473 cm^{-1}, 553 cm^{-1},689 cm^{-1} and 810 cm^{-1} are due to Mn-O present in the birnessite.

4.1.5 X-ray microprobe analysis - surface elemental mapping

Surface elemental mapping using X-ray microprobe analysis was performed to determine if the location of particular elements such as manganese and iron are correlated to specific locations on or inside the fossil bone matrix.

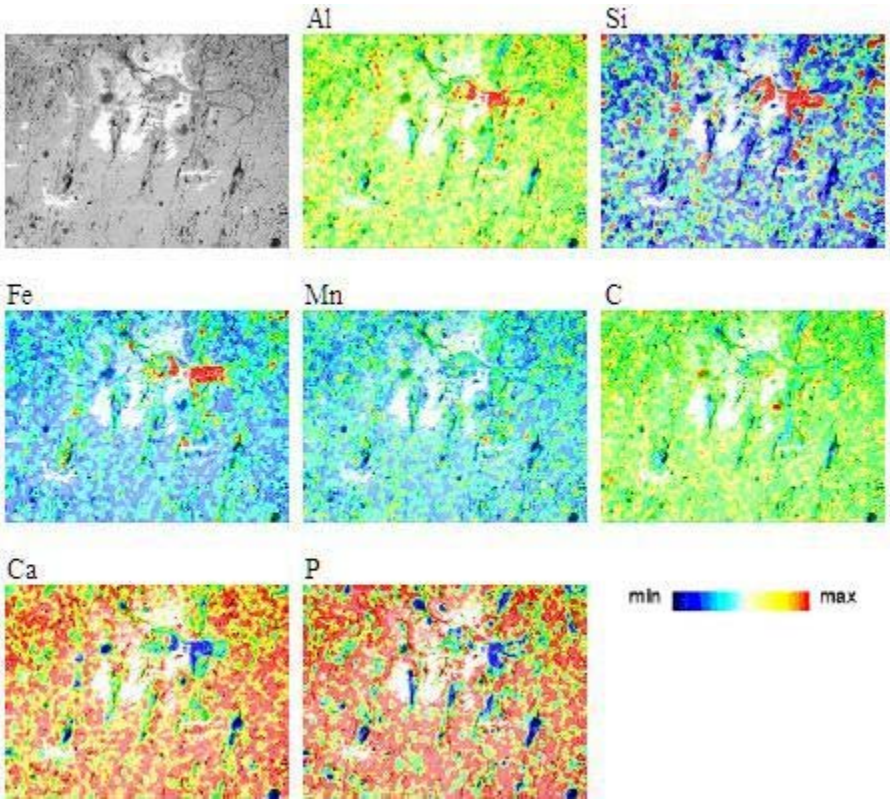

Figure 4.9 Optical image of bone target area and maps of the elemental distribution in the fossil bone fragment made by EPMA.

Testing with the use of an electron microprobe X-ray analyzer was performed for the chemical analysis of fossil bones by A. Kuczumow in the Department of Chemistry, Catholic University of Lublin, Poland. All results obtained as mappings show the distribution of elements detected within the sample (Figs. 4.9-4.10). Calcium and phosphorous signals were dominant, due to great intensity of fluorescent signals of the main elements. The signals approximately matched each other. Silicon and aluminium appears as a correlated pair of elements. The presence of iron (significantly obvious) and manganese (less obvious) was associated with the above mentioned aluminosilicate.

Furthermore the iron appears to show better penetration into the bulk of the sample compared to the manganese which is mainly located on the surface edges.

There seems to be no direct visible correlation with respect to the elemental distribution in the edge area of the sample (Fig. 4.9).

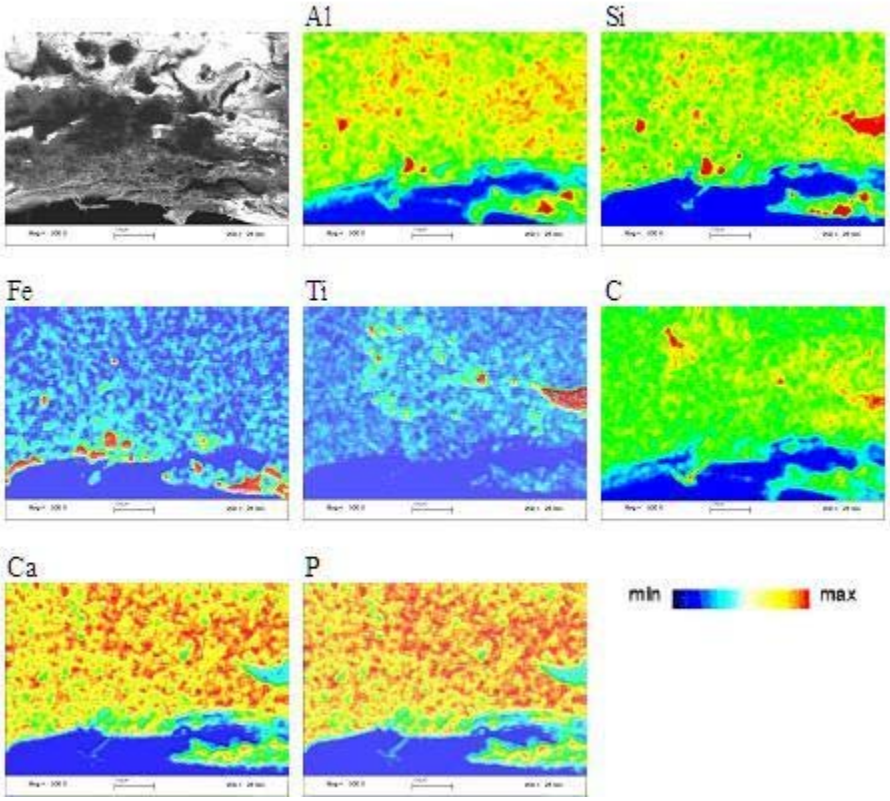

Figure 4.10 Optical image of bone target area and maps of the elemental distribution in the fossil bone fragment from EPMA.

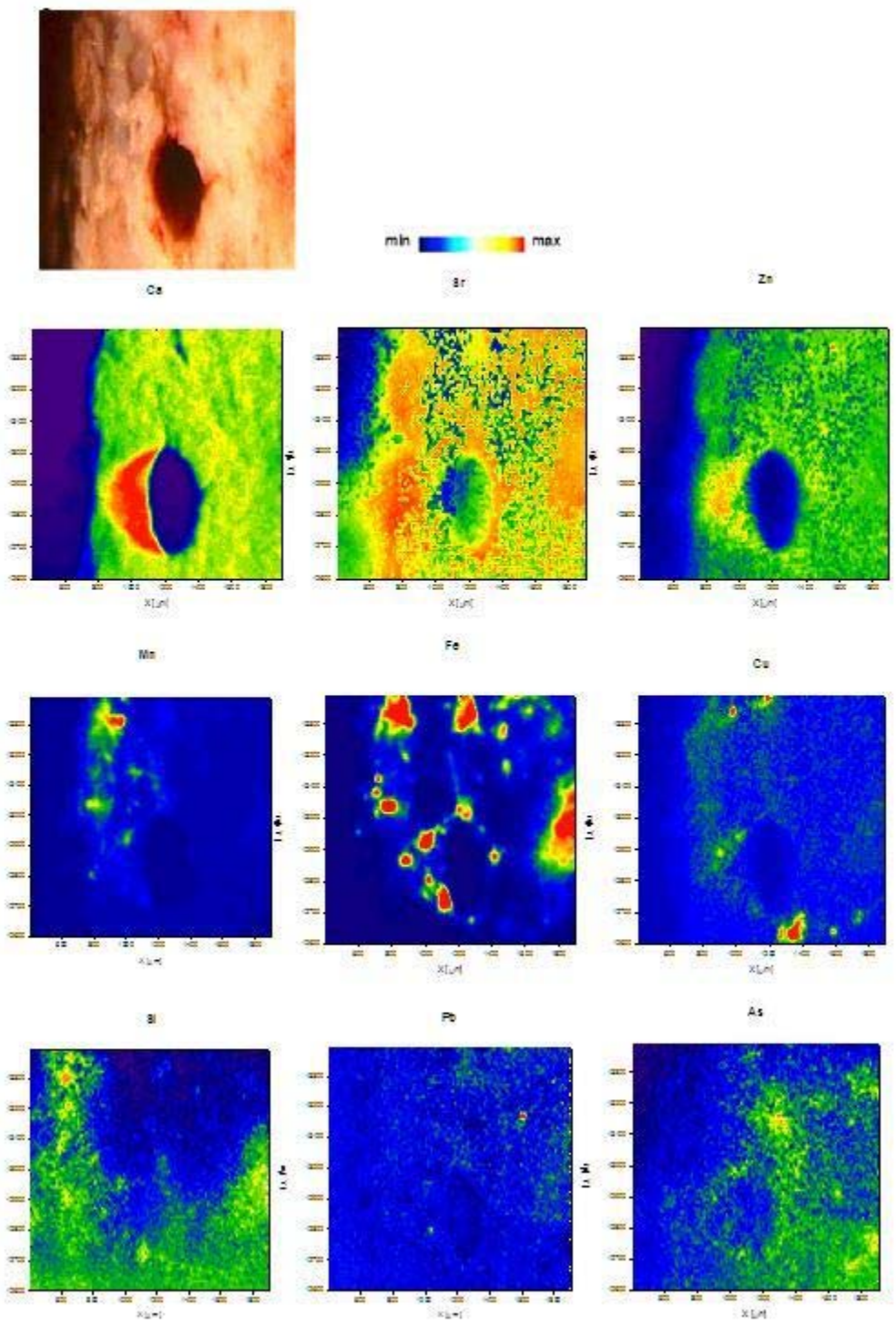

Figure 4.11 Optical image of bone target area and the elemental mappings of the fossil bone fragment made with synchrotron-based XRF: A) optical image; B) Ca; C) Sr; D) Zn; E) Mn; F) Fe; G) Cu; H) Si; I) Pb; J) As mappings.

(Fig. 4.11) The main heavier elements detected were: iron, manganese, zinc, copper, arsenic and lead. Calcium was detected throughout the bone as a matrix element. Manganese and copper were associated with iron, however, they were not found in all locations where iron was located. It is observed that manganese and copper were present in the edge zone of the bone whereas iron was also shown to penetrate into deeper areas of the bone matrix. Manganese and copper inclusions in the bone are not due to the bone's morphology but rather to overall bone porosity and random mechanical fracture of the edge. Iron and manganese had different distribution patterns. Iron showing deeper penetration into the bone matrix whereas manganese is mainly located on the surface and fissure edges.

4.1.6 X-ray fluorescence (XRF) analysis

Sample preparation was achieved by cutting each bone fragment into two pieces so as to expose a fresh cross sectional surface. The fragments were then plugged into modelling clay to hold them perpendicular to the X-ray beam.

Table 4.2 Measurement parameters used for XRF analysis of different manganese oxide coated fossil bone samples.

Measurement		
Target	Direct excitation	Direct excitation
Collimator/ mm	0.1	0.1
Spot size/ mm	0.2	0.2
Tube voltage/ kV	45	45
Measurement time/ s	60	10

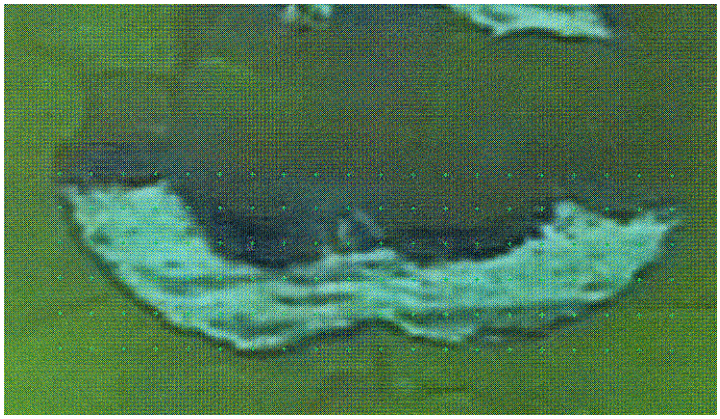

Figure 4.12 Optical image of across section of a manganese oxide coated fossil bone specimen. The green dots represent the target area of the analysis.

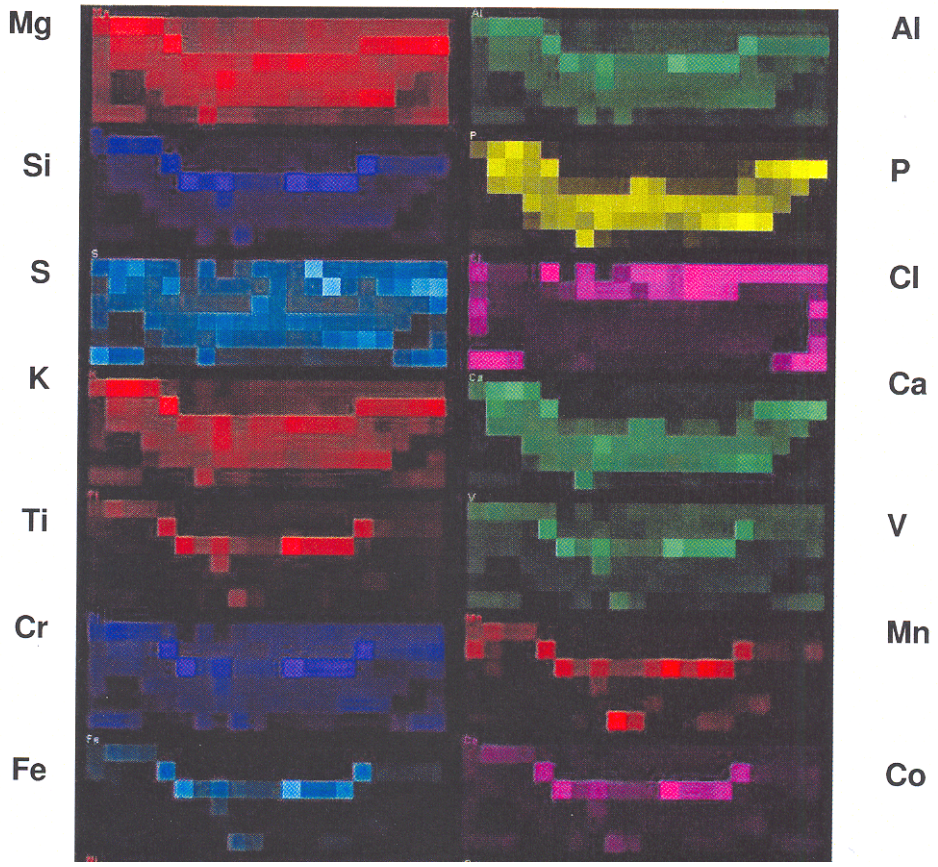

Figure 4.13 XRF image at 1 mm resolution of a cross section of a manganese oxide coated fossil bone fragment.

Iron, manganese, silicone and aluminum can be seen to occupy surface voids where phosphorous and calcium intensity is low. This is expected and is indicative of diagenetic and mineral leaching which has occurred at the bone surface.

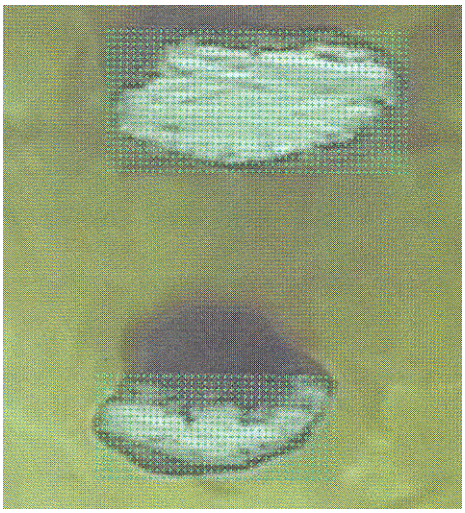

Figure 4.14 Optical image of a cross section of a manganese oxide coated fossil bone specimen. The green dots represent the analysis target area.

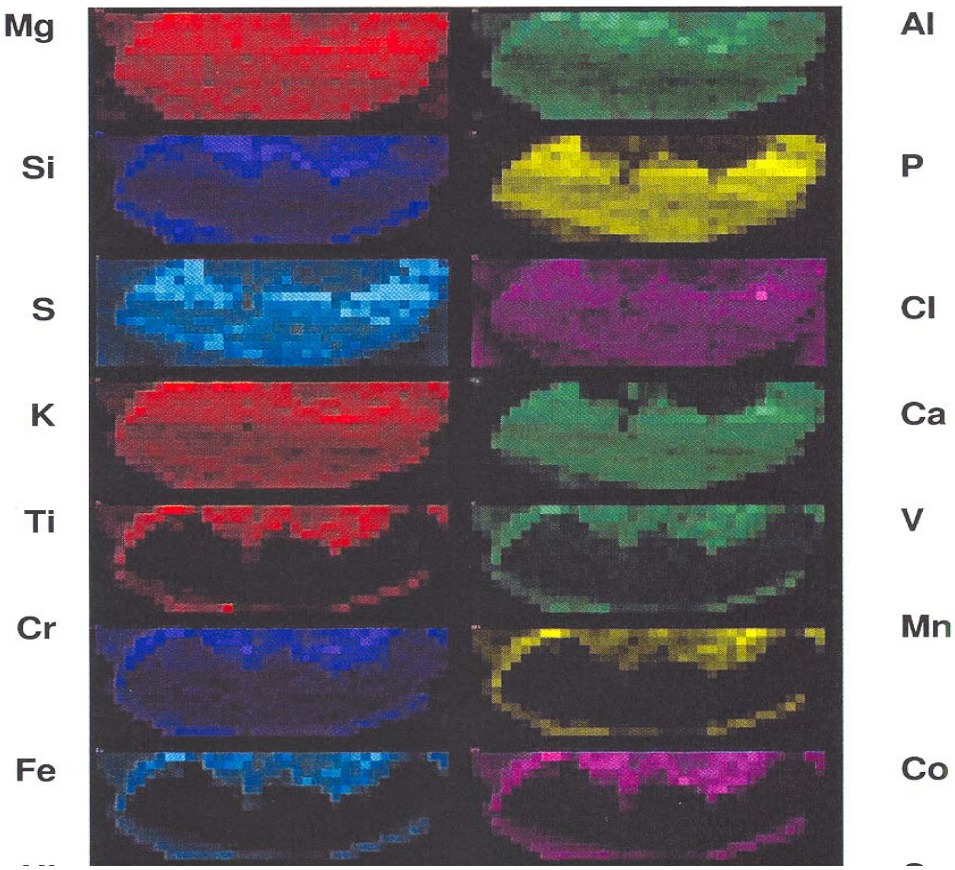

Figure 4.15 XRF image at 0.6 mm resolution of a cross section of a manganese oxide coated fossil bone fragment.

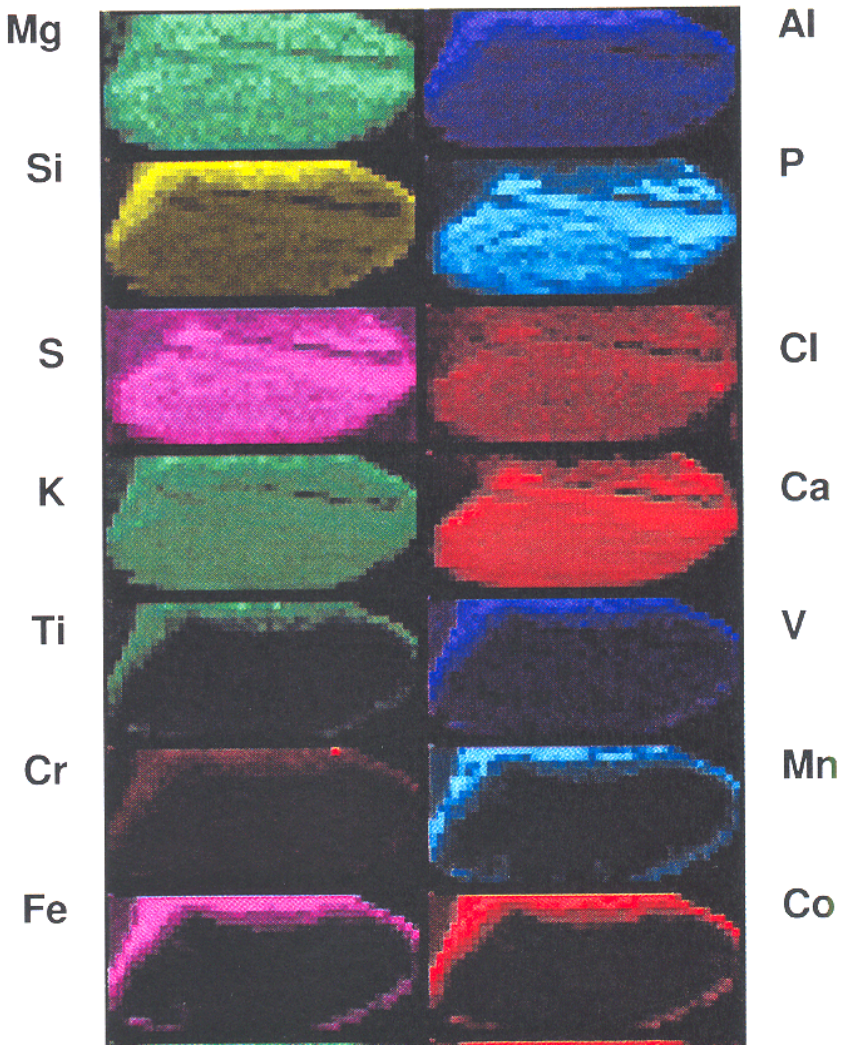

Figure 4.16 XRF image at 0.2mm resolution of a cross section of a manganese oxide coated fossil bone fragment.

The replacement of calcium and phosphorous at the surface edges of the manganese oxide coated fossil bone can be clearly seen and follows the same correlation for all three different manganese oxide coated fossil bone specimens. Manganese and iron appear as high intensities at the surface with iron showing a slightly higher intensity deeper into the surface layer of the bone.

For all the XRF images shown above, the brighter the colour the higher the X-ray intensity for that particular element. The different colours do not signify any significant difference between each element.

There appears to be a correlation between some elements and their intensities. Due to diagenesis various mineral elements have been replaced or removed from the bone surface and this is clearly observed in the image above. Calcium and phosphorous are of lower intensity at the same regions on the surface of the cross section where silicone and aluminium are high on the bone surface.